6924 *Inorg. Chem.* **2009**, *48*, 6924–6933
DOI: 10.1021/ic900391q

Inorganic Chemistry
Article

Bimetallic N-Heterocyclic Carbene−Iridium Complexes: Investigating Metal−Metal and Metal−Ligand Communication via Electrochemistry and Phosphorescence Spectroscopy

Andrew G. Tennyson, Evelyn L. Rosen, Mary S. Collins, Vincent M. Lynch, and Christopher W. Bielawski*

Department of Chemistry and Biochemistry, The University of Texas at Austin, 1 University Station A5300, Austin, Texas 78712

Received February 25, 2009

Bimetallic [Ir(COD)Cl] and [Ir(ppy)$_2$] (COD = 1,5-cyclooctadiene; ppy = 2-phenylpyridyl) complexes bridged by 1,7-dimethyl-3,5-diphenylbenzobis(imidazolylidene) (**1**), in addition to their monometallic analogues supported by 1-methyl-3-phenylbenzimidazolylidene (**2**), were synthesized and studied. Electrochemical analyses indicated that **1** facilitated moderate electronic coupling between [Ir(COD)Cl] units ($\Delta E = \sim$60 mV), but not [Ir(ppy)$_2$]. The metal-based oxidation potentials for the bimetallic complexes were within 20 mV of those for their monometallic analogues. Furthermore, spectroscopic analyses of the [Ir(ppy)$_2$] bimetallic and monometallic complexes revealed nearly identical phosphorescence profiles, indicating that carbene coordination does not affect the energy of the emissive states. Collectively, these results suggest that N-heterocyclic carbenes (NHCs) such as **1** could link together two emissive fragments without altering their fundamental phosphorescence profiles. Ultimately, employing multitopic NHCs as non-interfering molecular connectors could facilitate the rational design of new phosphorescent materials as well as second-generation phosphor dopants.

Introduction

Light emission from diodes was first observed nearly a century ago as an intellectual curiosity; however, this phenomenon did not find widespread commercial applications until many decades later.[1] Since then, light emitting diodes (LEDs) have become common in applications ranging from electroluminescent displays to data storage.[2] The simplest LEDs are diodes that emit light upon electron−hole recombination at a semiconductor p−n junction, as opposed to releasing energy as heat or in some other non-radiative form.[3,4] Not all semiconductors can emit, and in those that can, the emission wavelength is determined by the bandgap potential energy difference and thus cannot be easily modified.

Organic light-emitting diodes (OLEDs) are hybrid organic−inorganic devices that allow tuning of emission wavelength and lifetime without the need for new semiconductor designs.[5−9] Typically, an organic, π-conjugated polymer (CP) performs the conductor and emitter roles of the classical, inorganic LED. Tuning of CP spectroscopic and material properties can then be achieved via modification of the polymer's chemical components.[10,11] Electron−hole recombination results in singlet and triplet excitons; thus, device efficiency is enhanced by adding a phosphorescent component to the CP layer. Most phosphors are complexes of second and third-row transition metals, whose spin−orbit coupling enables emission from triplet excited states. Phosphor-functionalized OLEDs can be prepared by either physical doping of a CP with a phosphorescent inorganic complex[5,7] or via chemical incorporation of a similar moiety directly into a polymer chain to afford a conducting metallopolymer (CMP).[6,8,9] The majority of OLED devices comprise organic frameworks doped with phosphorescent iridium[12−15] or platinum[16] complexes. Iridium-based dopants are more attractive than those based on platinum, given the reactivity of the latter with water at high potentials to

*To whom correspondence should be addressed. E-mail: bielawski@cm.utexas.edu.

(1) Allen, J. W.; Grimmeiss, J. W. *Mater. Sci. Forum* **2008**, *590*, 1–16.
(2) Ponce, F. A.; Bour, D. P. *Nature* **1997**, *386*, 351–359.
(3) Craford, M. G. *MRS Bull.* **2000**, *25*, 27–31.
(4) Mitschke, U.; Bäuerle, P. *J. Mater. Chem.* **2000**, *10*, 1471–1507.
(5) Huang, S.-P.; Jen, T.-H.; Chen, Y.-C.; Hsiao, A.-E.; Yin, S.-H.; Chen, H.-Y.; Chen, S.-A. *J. Am. Chem. Soc.* **2008**, *130*, 4699–4707.
(6) Chan, W. K. *Coord. Chem. Rev.* **2007**, *251*, 2104–2118.
(7) Shirota, Y.; Kageyama, H. *Chem. Rev.* **2007**, *107*, 953–1010.
(8) Yamamoto, T.; Koizumi, T.-a. *Polymer* **2007**, *48*, 5449–5472.
(9) Sandee, A. J.; Williams, C. K.; Evans, N. R.; Davies, J. E.; Boothby, C. E.; Köhler, A.; Friend, R. H.; Holmes, A. B. *J. Am. Chem. Soc.* **2004**, *126*, 7041–7048.
(10) Holliday, B. J.; Swager, T. M. *Chem. Commun.* **2005**, 23–36.
(11) Kuroda, K.; Swager, T. M. *Macromolecules* **2004**, *37*, 716–724.
(12) You, Y.; Park, S. Y. *Dalton Trans.* **2009**, 1267–1282.
(13) Thompson, M. E. *MRS Bull.* **2007**, *32*, 694–701.
(14) Lowry, M. S.; Bernhard, S. *Chem.—Eur. J.* **2006**, *12*, 7970–7977.
(15) Li, J.; Djurovich, P. I.; Alleyne, B. D.; Yousufuddin, M.; Ho, N. N.; Thomas, J. C.; Peters, J. C.; Bau, R.; Thompson, M. E. *Inorg. Chem.* **2005**, *44*, 1713–1727.
(16) Baldo, M. A.; O'Brien, D. F.; You, Y.; Shoustikov, A.; Sibley, S.; Thompson, M. E.; Forrest, S. R. *Nature* **1998**, *359*, 151–154.

Published on Web 06/19/2009

form platinum oxide. Whereas CMPs are less common, their molecular structure is well-defined and allows for the rational design of materials, a feature not found in doped CPs.

The discovery of stable N-heterocyclic carbenes (NHCs) enabled access to robust organometallic complexes and polymers, many of which have been used in a broad range of applications.[17−22] Although there are a variety of well-characterized phosphorescent complexes comprising rhenium,[23] ruthenium,[24] iridium,[12,25−28] platinum,[29,30] and gold[31−35] centers supported by NHCs or diaminocarbenes (see Figure 1 for selected examples), to the best of our knowledge, multimetallic complexes or related CMPs are unknown. This omission is surprising in light of the detailed studies of polymers[36,37] and bimetallic complexes[38−46] linked by non-carbenoid ditopic ligands and their intrinsic phosphorescent characteristics.

We have recently developed new classes of bis(NHC)s that feature two diametrically opposed NHCs connected via a common aromatic linker. These compounds have enabled

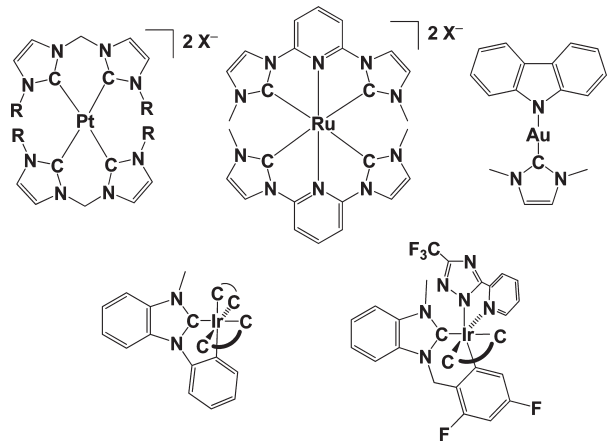

Figure 1. Representative phosphorescent NHC-based metal complexes.

the synthesis of unique bimetallic complexes,[47,48] as well as both organic[49−51] and organometallic[52−55] polymers, some of which were found to be conductive and luminescent. Given the synthetic modularity and electronic tunability inherent to the bis(NHC) scaffold and the existence of both heteroleptic NHC-based and bimetallic phosphors, we envisioned coordinating emissive components to this ditopic ligand. Subsequent analysis would probe how metal−metal and metal−ligand interactions could facilitate tuning of their respective electrochemical and luminescent properties.

Iridium(III) complexes bearing κ^2(N,C) heteroaromatic-aryl ligands have been thoroughly studied[12] by electrochemical as well as photophysical methods and have been widely used as dopants in OLED applications. Inspired by the seminal work of Thompson and co-workers with Ir complexes supported by ppy- and NHC- based ligands (ppy = 2-phenylpyridyl, NHC = 1-methyl-7-phenylbenzimidazolylidene; Figure 1),[13,15,28,56−62] we chose 1,7-dimethyl-3,5-diphenylbenzobis(imidazolylidene) (**1**) as a suitable ditopic linker

(17) Hahn, F. E.; Jahnke, M. C. *Angew. Chem., Int. Ed.* **2008**, *47*, 3122–3172.
(18) Lappert, M. F. *J. Organomet. Chem.* **2005**, *690*, 5467–5473.
(19) Peris, E.; Crabtree, R. H. *Coord. Chem. Rev.* **2004**, *248*, 2239–2246.
(20) Bourissou, D.; Guerret, O.; Gabbaï, F. P.; Bertrand, G. *Chem. Rev.* **2000**, *100*, 39–91.
(21) Arduengo, A. J.III *Acc. Chem. Res.* **1999**, *32*, 913–921.
(22) Herrmann, W. A.; Köcher, K. *Angew. Chem., Int. Ed. Engl.* **1997**, *36*, 2163–2187.
(23) Xue, W.-M.; Chan, M. C.-W.; Su, Z.-M.; Cheung, K.-K.; Liu, S.-T.; Che, C.-M. *Organometallics* **1998**, *17*, 1622–1630.
(24) Son, S. U.; Park, K. H.; Lee, Y.-S.; Kim, B. Y.; Choi, C. H.; Lah, M. S.; Jang, Y. H.; Jang, D.-J.; Chung, Y. K. *Inorg. Chem.* **2004**, *43*, 6896–6898.
(25) Tapu, D.; Owens, C.; VanDerveer, D.; Gwaltney, K. *Organometallics* **2009**, *28*, 270–276.
(26) Chang, C.-F.; Cheng, Y.-M.; Chi, Y.; Chiu, Y.-C.; Lin, C.-C.; Lee, G.-H.; Chou, P.-T.; Chen, C.-C.; Chang, C.-H.; Wu, C.-C. *Angew. Chem., Int. Ed.* **2008**, *47*, 4542–4545.
(27) Chien, C.-H.; Fujita, S.; Yamoto, S.; Hara, T.; Yamagata, T.; Watanabe, M.; Mashima, K. *Dalton Trans.* **2008**, 916–923.
(28) Sajoto, T.; Djurovich, P. I.; Tamayo, A.; Yousufuddin, M.; Bau, R.; Thompson, M. E.; Holmes, R. J.; Forrest, S. R. *Inorg. Chem.* **2005**, *44*, 7992–8003.
(29) Unger, Y.; Zeller, A.; Ahrens, S.; Strassner, T. *Chem. Commun.* **2008**, 3263–3265.
(30) Lai, S.-W.; Chan, M. C.-W.; Cheung, K.-K.; Che, C.-M. *Organometallics* **1999**, *18*, 3327–3336.
(31) Rios, D.; Pham, D. M.; Fettinger, J. C.; Olmstead, M. M.; Balch, A. L. *Inorg. Chem.* **2008**, *47*, 3442–3451.
(32) Bartolomé, C.; Carrasco-Rando, M.; Coco, S.; Cordovilla, C.; Espinet, P.; Martín-Alvarez, J. M. *Dalton Trans.* **2007**, 5339–5345.
(33) Wang, H. M. J.; Vasam, C. S.; Tsai, T. Y. R.; Chen, S.-H.; Chang, A. H. H.; Lin, I. J. B. *Organometallics* **2005**, *24*, 486–493.
(34) White-Morris, R. L.; Olmstead, M. M.; Jiang, F.; Tinti, D. S.; Balch, A. L. *J. Am. Chem. Soc.* **2002**, *124*, 2327–2336.
(35) Wang, H. M. J.; Chen, C. Y. L.; Lin, I. J. B. *Organometallics* **1999**, *18*, 1216–1223.
(36) Langecker, J.; Rehahn, M. *Macromol. Chem. Phys.* **2008**, *209*, 258–271.
(37) Kappaun, S.; Eder, S.; Sax, S.; Saf, R.; Mereiter, K.; List, E. J. W.; Slugovc, C. *J. Mater. Chem.* **2006**, *16*, 4389–4392.
(38) Whittle, V. L.; Williams, J. A. G. *Inorg. Chem.* **2008**, *47*, 6596–6607.
(39) Auffrant, A.; Barbieri, A.; Barigelletti, F.; Lacour, J.; Mobian, P.; Collin, J.-P.; Sauvage, J.-P.; Ventura, B. *Inorg. Chem.* **2007**, *46*, 6911–6919.
(40) Chen, L.; Yang, C.; Li, M.; Qin, J.; Gao, J.; You, H.; Ma, D. *Cryst. Growth Des.* **2007**, *7*, 39–46.
(41) Lafolet, F.; Welter, S.; Popović, Z.; Cola, L. D. *J. Mater. Chem.* **2005**, *15*, 2820–2828.
(42) Cicogna, F.; Gaddi, B.; Ingrosso, G.; Marcaccio, M.; Marchetti, F.; Paolucci, D.; Paolucci, F.; Pinzino, C.; Viglione, R. *Inorg. Chim. Acta* **2004**, *357*, 2915–2932.
(43) Tsuboyama, A.; Takiguchi, T.; Okada, S.; Osawa, M.; Hoshino, M.; Ueno, K. *Dalton Trans.* **2004**, 1115–1116.
(44) Neve, F.; Crispini, A.; Serroni, S.; Loiseau, F.; Campagna, S. *Inorg. Chem.* **2001**, *40*, 1093–1101.
(45) Carlson, G. A.; Djurovich, P. I.; Watts, R. J. *Inorg. Chem.* **1993**, *32*, 4483–4484.
(46) Winkler, J. R.; Marshall, J. L.; Netzel, T. L.; Gray, H. B. *J. Am. Chem. Soc.* **1986**, *108*, 2263–2266.
(47) Er, J. A. V.; Tennyson, A. G.; Kamplain, J. W.; Lynch, V. M.; Bielawski, C. W. *Eur. J. Inorg. Chem.* **2009**, 1729–1738.
(48) Khramov, D. M.; Boydston, A. J.; Bielawski, C. W. *Angew. Chem., Int. Ed.* **2006**, *45*, 6186–6189.
(49) Coady, D. J.; Norris, B. C.; Khramov, D. M.; Tennyson, A. G.; Bielawski, C. W. *Angew. Chem., Int. Ed.* **2009**, DOI: 10.1002/anie.200901046.
(50) Tennyson, A. G.; Kamplain, J. W.; Bielawski, C. W. *Chem. Commun.* **2009**, 2124–2126.
(51) Kamplain, J. W.; Bielawski, C. W. *Chem. Commun.* **2006**, 1727–1729.
(52) Williams, K. A.; Boydston, A. J.; Bielawski, C. W. *J. R. Soc. Interface* **2007**, *4*, 359–362.
(53) Boydston, A. J.; Rice, J. D.; Sanderson, M. D.; Dykhno, O. L.; Bielawski, C. W. *Organometallics* **2006**, *25*, 6087–6098.
(54) Boydston, A. J.; Bielawski, C. W. *Dalton Trans.* **2006**, 4073–4077.
(55) Boydston, A. J.; Williams, K. A.; Bielawski, C. W. *J. Am. Chem. Soc.* **2005**, *127*, 12496–12497.
(56) Hirani, B.; Li, J.; Djurovich, P. I.; Yousufuddin, M.; Oxgaard, J.; Persson, P.; Wilson, S. R.; Bau, R.; Goddard, W. A.III; Thompson, M. E. *Inorg. Chem.* **2007**, *46*, 3865–3875.
(57) Sun, Y.; Giebink, N. C.; Kanno, H.; Ma, B.; Thompson, M. E.; Forrest, S. R. *Nature* **2006**, *440*, 908–912.
(58) Holmes, R. J.; Forrest, S. R.; Sajoto, T.; Tamayo, A.; Djurovich, P. I.; Thompson, M. E.; Brooks, J.; Tung, Y.-J.; D'Andrade, B. W.; Weaver, M. S.; Kwong, R. C.; Brown, J. J. *Appl. Phys. Lett.* **2005**, *87*, 243507.
(59) Li, J.; Djurovich, P. I.; Alleyne, B. D.; Tsyba, I.; Ho, N. N.; Bau, R.; Thompson, M. E. *Polyhedron* **2004**, *23*, 419–428.
(60) Thompson, M. K.; Doble, D. M. J.; Tso, L. S.; Barra, S.; Botta, M.; Aime, S.; Raymond, K. N. *Inorg. Chem.* **2004**, *43*, 8577–8586.
(61) Tamayo, A. B.; Alleyne, B. D.; Djurovich, P. I.; Lamansky, S.; Tsyba, I.; Ho, N. N.; Bau, R.; Thompson, M. E. *J. Am. Chem. Soc.* **2003**, *125*, 7377–7387.
(62) Lamansky, S.; Djurovich, P.; Murphy, D.; Abdel-Razzaq, F.; Kwong, R.; Tsyba, I.; Bortz, M.; Mui, B.; Bau, R.; Thompson, M. E. *Inorg. Chem.* **2001**, *40*, 1704–1711.

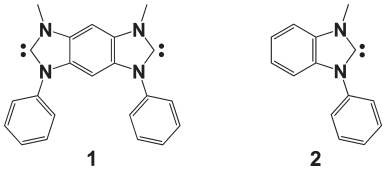

Figure 2. Structures of **1** and **2**.

for our studies (Figure 2). Because the degree of electronic communication across a linking scaffold can be conveniently measured via electrochemical analysis of coordinated redox active centers,[63,64] our initial efforts focused on preparing and studying bimetallic bis(NHC) complexes affixed to [Ir(COD)Cl] (COD = 1,5-cyclooctadiene) moieties. Additionally, many complexes of this type have been crystallographically characterized,[63,65−73] allowing for greater comparison and interpretation of metric parameters. Building on this foundation, we pursued the synthesis and photoluminescent characterization of bimetallic Ir complexes bearing ppy ligands. To gain greater insight into the fundamental interactions inherent to the aforementioned bis(NHC) complexes, monometallic analogues supported by 1-methyl-3-phenylbenzimidazolylidene (**2**) were synthesized and studied in parallel.

Experimental Section

Materials and Methods. Iridium trichloride hydrate and $[Ir(COD)(\mu-Cl)]_2$ were purchased from Strem Chemicals. 2-Methyltetrahydrofuran (MeTHF) was purchased from Aldrich. Dichloromethane (CH_2Cl_2) was distilled from CaH_2. Solvents were degassed by three consecutive freeze−pump−thaw cycles. 1,7-Diphenyl-benzobisimidazole,[74] $[\mathbf{1}H_2][MeSO_4]_2$,[74] and $[Ir(ppy)_2(\mu-Cl)]_2$[62,75] were synthesized as previously described. Compounds [**2**H][I],[53] **5**,[28] and **6**[28] were prepared by following literature procedures with minor modifications (vide infra). All other materials and solvents were of reagent quality and used as received. ^1H and ^{13}C $\{^1H\}$ NMR spectra were recorded using a Varian 300, 400, 500, or 600 MHz spectrometer. Chemical shifts δ (in ppm) are referenced to tetramethylsilane using the residual solvent as an internal standard. For ^1H NMR: $CDCl_3$, 7.24 ppm; DMSO-d_6, 2.49 ppm. For ^{13}C NMR: $CDCl_3$, 77.0 ppm; DMSO-d_6, 39.5 ppm. Coupling constants are expressed in hertz (Hz). High-resolution mass spectra (HRMS) were obtained with a VG analytical ZAB2-E instrument (ESI or CI). Elemental analyses were performed at Midwest Microlab, LLC, Indianapolis, IN and Columbia Analytical Services, Tucson, AZ. Whereas complexes **3**−**6** were prepared under an N_2 atmosphere using drybox or Schlenk techniques, all other syntheses were performed under ambient conditions.

Electrochemistry. Electrochemical experiments were conducted on CH Instruments Electrochemical Workstations (series 630B and 700B) using a gastight, three-electrode cell under an atmosphere of dry nitrogen. The cell was equipped with platinum working and counter electrodes, as well as a silver wire quasi-reference electrode. Measurements were performed in dry CH_2Cl_2 with 0.1 M [tetra-*n*-butylammonium][PF_6] as the electrolyte and decamethylferrocene [Fc*] as the internal standard. Chronoamperometry experiments were performed using a 30 μm diameter Pt ultramicroelectrode as the working electrode. Complexes **3**−**6** displayed irreversible electrochemical behavior at all scan rates examined (50 mV s^{-1} to 5 V s^{-1}). All potentials listed in the manuscript and the Experimental Section were determined at 100 mV s^{-1} scan rates and referenced to SCE by shifting $[Fc^*]^{0/+}$ to −0.057 V.[76]

General Spectroscopic Considerations. UV−visible absorption and fluorescence emission spectra were recorded on a Perkin-Elmer Lambda 35 spectrometer and a PTI Quanta-Master 4 L fluorimeter, respectively. All room-temperature measurements were made using matched 6Q Spectrosil quartz cuvettes (Starna) with 1 cm path lengths and 3.0 mL of sample solution volumes. Measurements at 77 K were performed in 5 mm diameter quartz tubes with 0.3 mL sample solution volumes. Absorption and emission spectra were acquired in water under ambient conditions for $[\mathbf{1}H_2][MeSO_4]_2$ and [**2**H][$MeSO_4$] or in MeTHF under N_2 atmosphere for complexes **3**−**6**. Extinction coefficients (ε) were determined from Beer's law measurements using 10, 20, 30, and 40 μM concentrations of the analyte. Emission spectra were acquired using 1.0 μM solutions of chromophore. Room-temperature quantum yields were determined relative to 1.0 μM quinine sulfate in 0.1 *N* H_2SO_4.[77] Quantum yields at 77 K were estimated assuming k_r was temperature-independent and using $\Phi^{77} = k_r\tau$.[77]

Syntheses. [3,5-Dimethyl-1,7-diphenylbenzobis(imidazolium)]-[I]$_2$ [1H$_2$][I]$_2$. A solution of 1,7-diphenylbenzobisbenzimidazole[74] (605 mg, 1.95 mmol) in 15 mL of CH_3CN was charged with CH_3I (650 mg, 4.58 mmol) and then heated to 95 °C in a heavy-walled reaction flask equipped with a gastight Teflon cap, resulting in gradual formation of a precipitate. After 5 h, the mixture was allowed to cool to room temperature. The precipitate was then collected via vacuum filtration and then recrystallized from refluxing methanol to afford 803 mg (1.78 mmol, 91% yield) of the desired product as pale yellow crystals. ^1H NMR (500 MHz, DMSO-d_6): δ 10.41 (s, 2H), 9.12 (s, 1H), 8.05 (s, 1H), 7.90 (d, J = 8.1, 4H), 7.79−7.70 (m, 6H), 4.30 (s, 6H). ^{13}C NMR (100 MHz, DMSO-d_6): δ 146.9, 132.9, 131.1, 130.6, 130.4, 130.0, 125.2, 99.9, 97.8, 34.6. HRMS Calcd for $C_{22}H_{20}N_4$ ($[M^{2+}] \div 2$): 170.0839. Found 170.08385.

N-Phenyl-2-nitroaniline. 1-Fluoro-2-nitrobenzene (1.82 g, 8.38 mmol) and aniline (1.56 g, 16.8 mmol) were dissolved in 15 mL of isopropanol and then heated to 115 °C in a heavy-walled reaction flask equipped with a gastight Teflon cap. After 48 h, the solution was allowed to cool to room temperature and then filtered to remove residual solids. The filtrate was then concentrated under reduced pressure to afford a red oil, which was purified using column chromatography (SiO_2, 5:1 hexanes/ethyl

(63) Leuthäusser, S.; Schwarz, D.; Plenio, H. *Chem.—Eur. J.* **2007**, *13*, 7195–7203.
(64) Zanello, P. *Inorganic Electrochemistry: Theory, Practice and Application*; The Royal Society of Chemistry: Cambridge, 2003.
(65) Kelly, R. A.III; Clavier, H.; Giudice, S.; Scott, N. M.; Stevens, E. D.; Bordner, J.; Samardjiev, I.; Hoff, C. D.; Cavallo, L.; Nolan, S. P. *Organometallics* **2008**, *27*, 202–210.
(66) Kownacki, I.; Kubicki, M.; Szubert, K.; Marciniec, B. *J. Organomet. Chem.* **2008**, *693*, 321–328.
(67) Chen, D.; Banphavichit, V.; Reibenspies, J.; Burgess, K. *Organometallics* **2007**, *26*, 855–859.
(68) Iglesias, M.; Beetstra, D. J.; Stasch, A.; Horton, P. N.; Hursthouse, M. B.; Coles, S. J.; Cavell, K. J.; Dervisi, A.; Fallis, I. A. *Organometallics* **2007**, *26*, 4800–4809.
(69) Herrmann, W. A.; Baskakov, D.; Herdtweck, E.; Hoffmann, S. D.; Bunlaksananusorn, T.; Rampf, F.; Rodefeld, L. *Organometallics* **2006**, *25*, 2449–2456.
(70) Viciano, M.; Poyatos, M.; Sanaú, M.; Peris, E.; Rossin, A.; Ujaque, G.; Lledós, A. *Organometallics* **2006**, *25*, 1120–1134.
(71) Vicent, C.; Viciano, M.; Mas-Marzá, E.; Sanaú, M.; Peris, E. *Organometallics* **2006**, *25*, 3713–3720.
(72) Chianese, A. R.; Li, X.; Janzen, M. C.; Faller, J. W.; Crabtree, R. H. *Organometallics* **2003**, *22*, 1663–1667.
(73) Seo, H.; Kim, B. Y.; Lee, J. H.; Park, H.-J.; Son, S. U.; Chung, Y. K. *Organometallics* **2003**, *22*, 4783–4791.
(74) Boydston, A. J.; Pecinovsky, C. S.; Chao, S. T.; Bielawski, C. W. *J. Am. Chem. Soc.* **2007**, *129*, 14550–14551.
(75) Nonoyama, M. *Bull. Chem. Soc. Jpn.* **1974**, *47*, 767–768.
(76) Noviandri, I.; Brown, K. N.; Fleming, D. S.; Gulyas, P. T.; Lay, P. A.; Masters, A. F.; Phillips, L. *J. Phys. Chem. B* **1999**, *103*, 6713–6722.
(77) Melhuish, W. H. *J. Phys. Chem.* **1961**, *65*, 229–235.

acetate) to afford 1.08 g (5.04 mmol, 60% yield) of the desired product as a bright red oil that crystallizes upon standing. Spectral data were consistent with reported literature values.[78]

1-Phenylbenzimidazole. N-phenyl-2-nitroaniline (400 mg, 1.87 mmol), sodium formate (430 mg, 6.3 mmol), and Pd/C (10 mol %, 160 mg, 1.5 mmol) were suspended in 15 mL of formic acid (88%) and then heated to reflux. After 18 h, the reaction was allowed to cool to room temperature and then filtered through Celite with the aid of 20 mL of H_2O. The filtrate was then concentrated to 10 mL under reduced pressure, and the remaining solution was neutralized by slow addition of sat. Na_2CO_3 (aq). The product was then extracted from the aqueous solution with CH_2Cl_2 (2×15 mL). The combined organic fractions were dried with Na_2SO_4, filtered, and then concentrated under reduced pressure to afford 302 mg (1.55 mmol, 83% yield) of the desired product as a brown oil that needed no additional purification. Spectral data were consistent with reported literature values.[79]

[1-Methyl-3-phenylbenzimidazolium][I] [2H][I]. A solution of 1-phenylbenzimidazole (177 mg, 0.913 mmol) in 10 mL of CH_3CN was charged with CH_3I (213 mg, 1.50 mmol) and then heated to 95 °C in a heavy-walled reaction flask equipped with a gastight Teflon cap. After 18 h, the solution was allowed to cool to room temperature. The solvent was then removed under reduced pressure, and the resulting residue was then triturated with Et_2O to give a yellow powder. Recrystallization of this crude material from refluxing methanol afforded 232 mg (0.690 mmol, 76% yield) of the desired product as light tan crystals. ^{1}H NMR (400 MHz, $CDCl_3$): δ 11.03 (s, 1H), 7.89−7.84 (m, 2H), 7.82−7.78 (m, 1H), 7.74−7.62 (m, 6H), 4.45 (s, 3H). ^{1}H NMR (300 MHz, DMSO-d_6): δ 10.18 (s, 1H), 8.17 (d, $J = 8.1$, 1H), 7.87−7.70 (m, 8H), 4.19 (s, 3H). ^{13}C NMR (75 MHz, DMSO-d_6): δ 143.0, 133.1, 131.8, 130.8, 130.4, 127.3, 126.8, 125.0, 113.9, 113.2, 33.6. HRMS Calcd for $C_{14}H_{13}N_2$ [M^+]: 209.1075. Found: 209.10732.

[1-Methyl-3-phenylbenzimidazolium][$MeSO_4$] [2H][$MeSO_4$]. A solution of [**2**H][I] (332 mg, 0.988 mmol) in 5 mL of CH_3CN was charged with Me_2SO_4 (100 μL, 1.0 mmol) and then heated to 70 °C. After 8 h, the solution was allowed to cool to room temperature. The solvent was then removed under reduced pressure, and the resulting residue was triturated with ethyl acetate to afford 298 mg (0.930 mmol, 94%) of the desired product as a gray powder. ^{1}H NMR (500 MHz, DMSO-d_6): δ 10.11 (s, 1H), 8.15 (d, $J = 8.0$, 1H), 7.85−7.82 (m, 3H), 7.81−7.71 (m, 5H), 4.18 (s, 3H), 3.34 (s, 3H). ^{13}C NMR (100 MHz, DMSO-d_6): δ 143.2, 133.2, 131.9, 130.9, 130.5, 127.4, 126.9, 125.1, 114.0, 113.3, 52.8, 33.5. HRMS Calcd for $C_{14}H_{13}N_2$ [M^+]: 209.1077. Found: 209.1079. UV−vis: λ_{max} = 269 nm, $\varepsilon = 1.00 \times 10^4$ M^{-1} cm^{-1}. Fluorescence: $\lambda_{em} = 396$ nm, $\Phi = 0.046$.

[{Ir(COD)Cl}$_2$(1)] (3). A solution of $NaN(SiMe_3)_2$ (117 mg, 0.638 mmol), $[Ir(COD)(\mu-Cl)]_2$ (185 mg, 0.275 mmol) in 15 mL of THF was charged with [**1**H_2][$MeSO_4$]$_2$ (150 mg, 0.267 mmol) and then stirred at room temperature for 12 h. Removal of solvent under reduced pressure afforded a crude product as a brown solid. Purification by column chromatography (SiO_2, 9:1 DCM/Et_2O) afforded 61 mg (60 μmol, 22% yield) of the desired product as a yellow solid. ^{1}H NMR (400 MHz, $CDCl_3$): δ 7.87 (br s, 4H), 7.56−7.44 (m, 6H), 7.23 (s, 1H), 7.07 (s, 1H), 4.76−4.68 (br m, 2H), 4.64−4.54 (br m, 2H), 4.32 (s, 6H), 3.04−2.96 (br m, 2H), 2.34−2.12 (m, 6H), 1.82−1.50 (m, 8H), 1.28−1.18 (m, 4H). ^{13}C (100 MHz, $CDCl_3$): δ 194.2, 137.5, 132.73, 132.67, 132.4, 132.3, 129.0, 128.6, 128.5, 127.4, 91.9, 91.8, 90.1, 87.3, 87.0, 86.33, 86.26, 52.52, 52.49, 52.3, 52.2, 35.1, 34.1, 34.0, 32.3, 29.2, 29.1, 29.0, 28.9. HRMS Calcd for $C_{38}H_{42}Cl_2N_4Ir_2$ [M^+]: 1010.2027. Found: 1010.20395. Anal. Calcd for $C_{38}H_{42}Cl_2N_4Ir_2$: C, 45.18; H, 4.19; N, 5.55. Found: C, 45.45; H, 3.95; N, 5.49. UV−vis: $\lambda_{max} = 338$ nm, $\varepsilon = 1.12 \times 10^4$ M^{-1} cm^{-1}.

[Ir(COD)(Cl)(2)] (4).[80] A solution of $NaN(SiMe_3)_2$ (27 mg, 0.15 mmol), $[Ir(COD)(\mu-Cl)]_2$ (50 mg, 74 μmol) in 5 mL of THF was charged with [**2**H][$MeSO_4$] (48 mg, 0.15 mmol) and then stirred at room temperature for 12 h. Removal of the solvent under reduced pressure afforded the crude product as a brown solid. Purification by column chromatography (SiO_2, 1:1 hexanes/ethyl acetate) afforded 63 mg (0.12 mmol, 78% yield) of the desired product as a yellow solid. ^{1}H NMR (400 MHz, $CDCl_3$): δ 7.96 (d, $J = 7.2$, 2H), 7.58−7.46 (m, 3H), 7.35 (d, $J = 7.6$, 1H), 7.29 (t, $J = 7.8$, 2H), 7.20 (t, $J = 7.2$, 1H), 4.73−4.68 (m, 1H), 4.60−4.55 (m, 1H), 4.25 (s, 3H), 2.97−2.93 (m, 1H), 2.36−2.31 (m, 1H), 2.25−2.10 (m, 2H), 1.85−1.73 (m, 1H), 1.70−1.52 (m, 3H), 1.34−1.22 (m, 2H). ^{13}C NMR (100 MHz, $CDCl_3$): δ 191.5, 137.7, 135.4, 135.2, 128.8, 128.2, 127.3, 123.1, 122.8, 110.5, 109.6, 86.4, 85.6, 52.3, 52.1, 34.6, 34.0, 32.3, 29.2, 29.0. HRMS Calcd for $C_{22}H_{24}N_2ClIr$ [M^+]: 544.1257. Found 544.1248. Anal. Calcd for $C_{22}H_{24}ClIrN_2$: C, 48.56; H, 4.45; N, 5.15. Found: C, 48.46; H, 4.52; N, 5.02. UV−vis: $\lambda_{max} = 302$ nm, $\varepsilon = 1.38 \times 10^4$ M^{-1} cm^{-1}. CCDC: 721646.[81]

[{Ir(ppy)$_2$}$_2$(1)] (5). A solution of [**1**H_2][I]$_2$ (134 mg, 0.226 mmol), Ag_2O (174 mg, 0.752 mmol) and $[Ir(ppy)_2(\mu-Cl)]_2$ (184 mg, 0.176 mmol) in 10 mL of 1,2-dichloroethane was heated to 95 °C in the dark. After 24 h, the solution was allowed to cool to room temperature and then filtered through Celite with the aid of 15 mL CH_2Cl_2. Removal of the solvent under reduced pressure afforded the crude product as a yellow solid. Purification by column chromatography (SiO_2, 9:1 CH_2Cl_2/Et_2O) afforded 76 mg (57 μmol, 33% yield) of the desired product as a yellow solid. ^{1}H NMR (600 MHz, $CDCl_3$): δ 9.01 (2 overlapping s, 1H), 8.08 (d, $J = 6.3$, 1H), 8.06 (d, $J = 5.4$, 1H), 7.96 (d, $J = 8.1$, 2H), 7.90 (d, $J = 6.0$, 1H), 7.82 (d, $J = 6.0$, 1H), 7.79−7.72 (m, 4H), 7.68−7.58 (m, 4H), 7.49−7.43 (m, 2H), 7.41−7.36 (m, 2H), 7.18 (t, $J = 7.2$, 2H), 6.95−6.82 (m, 13H), 6.70 (t, $J = 7.2$, 2H), 6.65 (t, $J = 6.6$, 1H), 6.63 (t, $J = 6.6$, 1H), 6.53 (t, $J = 6.6$, 1H), 6.50 (t, $J = 6.6$, 1H), 6.35 (t, $J = 6.8$, 2H), 3.35 (2 overlapping s, 6H). ^{13}C NMR (150 MHz, $CDCl_3$): δ 191.9, 191.8, 172.6, 172.26, 172.25, 169.92, 169.89, 168.73, 168.72, 156.74, 156.70, 153.09, 153.01, 152.3, 152.2, 150.1, 144.17, 144.16, 143.02, 143.00, 139.1, 134.8, 134.3, 134.2, 133.2, 133.06, 133.05, 130.3, 130.2, 129.6, 129.3, 125.5, 125.4, 124.3, 124.0, 121.9, 121.83, 121.80, 121.61, 121.57, 120.0, 119.0, 118.5, 111.9, 93.54, 93.51, 90.54, 90.49, 33.7. HRMS Calcd for $C_{66}H_{48}N_8Ir_2$ ([M^{2+}] ÷ 2): 669.1620. Found: 669.16247. Anal. Calcd for $C_{66}H_{48}Ir_2N_8$: C, 59.26; H, 3.62; N, 8.38. Found: C, 58.95; H, 3.52; N, 8.19. UV−vis: $\lambda_{max} = 343$ nm, $\varepsilon = 2.95 \times 10^4$ M^{-1} cm^{-1}. Fluorescence at 298 K: $\lambda_{em} = 497$ nm, $\Phi = 0.11$, $\tau = 0.79$ μs, $k_r = 1.7 \times 10^5$ s^{-1}, $k_{nr} = 1.1 \times 10^6$ s^{-1}. At 77 K: $\lambda_{em} = 482$ nm, $\Phi = 0.45$, $\tau = 3.4$ μs, $k_{nr} = 1.6 \times 10^5$ s^{-1}.

[Ir(ppy)$_2$(2)] (6).[82] Compound [**2**H][I] (48 mg, 0.14 mmol), Ag_2O (60 mg, 0.26 mmol), and $[Ir(ppy)_2(\mu-Cl)]_2$ (60 mg, 56 μmol) were dissolved in 10 mL of 1,2-dichloroethane; the reaction was heated to 90 °C in the dark. After 16 h, the solution was allowed to cool to room temperature and filtered through Celite with the aid of 10 mL of CH_2Cl_2. Removal of solvent under reduced pressure afforded the crude product as a yellow powder. Pur-

(78) Rao, H.; Jin, Y.; Fu, H.; Jiang, Y.; Zhao, Y. *Chem.—Eur. J.* **2006**, *12*, 3636–3646.

(79) Xie, Y.-X.; Pi, S.-F.; Wang, J.; Yin, D.-L.; Li, J.-H. *J. Org. Chem.* **2006**, *71*, 8324–8327.

(80) Fuchs, E.; Egen, M.; Kahle, K.; Lennartz, C.; Molt, O.; Nord, S.; Kowalsky, W.; Schildknecht, C.; Johannes, H.-H. Patent: WO 2007115970, October 18, **2007**.

(81) X-ray crystal structure data was collected for **4** and **6** (CCDC 721646 and 721647, respectively) and deposited with the Cambridge Crystallographic Data Centre, 12 Union Road, Cambridge CB2 1EZ, U.K.

(82) Thompson, M. E.; Tamayo, A.; Djurovich, P.; Sajoto, T.; Forrest, S. R.; Mackenzie, P. B.; Walters, R.; Brooks, J.; Li, X.-C.; Alleyne, B.; Tsai, J.-Y.; Lin, C.; Ma, B.; Barone, M. S.; Kwong, R. Patent: WO 2005113704, January 12, **2005**.

ification by column chromatography (SiO_2, 3:1 hexanes/ethyl acetate) afforded 55 mg (78 μmol, 69% yield) of the desired product as a yellow solid. ^{1}H NMR (400 MHz, $CDCl_3$): δ 8.22 (d, J=8.3, 1H), 8.09 (d, J=5.6, 1H), 7.92 (d, J=5.6, 1H), 7.90 (d, J=8.0, 1H), 7.82 (d, J=8.0, 1H), 7.76 (d, J=8.0, 1H), 7.72 (d, J=7.1, 1H), 7.67 (d, J=8.3, 1H), 7.51 (t, J=7.1, 1H), 7.43 (t, J=7.1, 1H), 7.38 (t, J=6.6, 1H), 7.31−7.27 (m, 2H), 7.08 (t, J=6.8, 1H), 6.95−6.86 (m, 6H), 6.74 (d, J=6.8, 1H), 6.68 (t, J=6.1, 1H), 6.60 (t, J = 6.1, 1H), 6.40 (d, J = 8.3, 1H), 3.39 (s, 3H). ^{13}C NMR (100 MHz, $CDCl_3$): δ 186.8, 170.2, 170.0, 167.5, 166.3, 154.6, 151.1, 150.5, 148.3, 142.4, 141.4, 137.3, 135.1, 133.2, 132.6, 131.6, 131.5, 128.9, 128.2, 127.9, 123.9, 123.0, 122.7, 121.9, 120.8, 120.7, 120.4, 118.7, 117.8, 117.3, 111.2, 110.6, 109.2, 34.5. HRMS Calcd for $C_{36}H_{28}IrN_4$ [M^+]: 709.1947. Found: 709.19377. Anal. Calcd for $C_{36}H_{28}IrN_4$: C, 61.00; H, 3.98; N, 7.90. Found: C, 61.18; H, 3.89; N, 7.88. UV−vis: λ_{max} = 258 nm, $\varepsilon = 5.13 \times 10^4$ M^{-1} cm^{-1}. Fluorescence at 298 K: λ_{em} = 497 nm, Φ = 0.19, τ = 0.69 μs, $k_r = 2.8\times10^5$ s^{-1}, $k_{nr} = 1.2\times10^6$ s^{-1}. At 77 K: λ_{em} = 482 nm, Φ = 0.87, τ = 3.0 μs, $k_{nr} = 4.4\times10^4$ s^{-1}. CCDC: 721647.[81]

Results and Discussion

N-Heterocyclic carbenes **1** and **2** cannot be isolated in their free forms because of polymerization[51] or dimerization side reactions,[83] and were therefore generated in situ from their respective benzimidazolium precursors. The requisite iodide salts of [**1**H_2] and [**2**H] were synthesized via alkylation of 1,7-diphenylbenzobis(imidazole)[74] or 1-phenylbenzimidazole,[79] respectively, with CH_3I in CH_3CN in good isolated yields (>75%). Upon methylation, the diagnostic ^{1}H signals for the 2,2′-positions shifted downfield from δ = 8.14 ppm in the benzobis(imidazole) precursor to 10.41 ppm (DMSO-d_6) in [**1**H_2][I]$_2$. Similarly, the ^{1}H peaks for the 2-position in the benzimidazole precursor shifted from δ = 8.13 to 11.03 ppm ($CDCl_3$) in [**2**H][I]. These changes are consistent with the addition of positive charge to the respective π systems.

Deprotonation of [**1**H_2][I]$_2$ or [**2**H][I] with $NaN(SiMe_3)_2$ in the presence of [Ir(COD)(μ−Cl)]$_2$ gave a mixture of complexes comprising both [Ir(COD)Cl] and [Ir(COD)I] fragments. To preclude halide scrambling with the Ir precursor, compounds [**1**H_2][$MeSO_4$]$_2$ and [**2**H][$MeSO_4$] were prepared by treating the corresponding iodide salts with Me_2SO_4.[84] Alternatively, these benzimidazolium salts could also be prepared via direct alkylation of the appropriate imidazole precursor with Me_2SO_4.[74] The ^{1}H NMR spectra for these benzimidazoliums are sensitive to the nature of the counterion.[84] For example, the protons at the 2,2′- or 2-positions in [**1**H_2][$MeSO_4$]$_2$ and [**2**H][$MeSO_4$] were shifted relatively upfield (δ = 10.41 to 10.37 ppm and 10.18 to 10.11 ppm in DMSO-d_6, respectively) compared to their iodide analogues. These changes are consistent with the higher affinity of the "hard" methysulfates for the benzimidazolium cation than the "soft" iodides in the respective salts.

As shown in Scheme 1, deprotonation of the methylsulfate salts with $NaN(SiMe_3)_2$ in the presence of [Ir(COD)(μ−Cl)]$_2$ afforded the desired complexes [{Ir(COD)Cl}$_2$(**1**)] (**3**) and [Ir(COD)Cl(**2**)] (**4**), respectively, in moderate to good yields. With complex **3**, the ^{1}H signals for the 2,2′-positions had disappeared and distinct multiplets from the olefinic COD protons were observed at δ = 4.72 and 4.60 ppm ($CDCl_3$), respectively. In addition, the ^{13}C NMR signal for the 2,2′-position for [**1**H_2][$MeSO_4$]$_2$ had dramatically shifted downfield to 194.2 ppm for **3**, consistent with the formation of a metal-bound NHC. Similar behavior was noted for **4** with nearly identical olefinic multiplets appearing at δ = 4.71 and 4.56 ppm and a significant downfield shift in the ^{13}C peak for the 2-position in [**2**H][$MeSO_4$] to 191.5 ppm in **4**. The diagnostic ^{1}H and ^{13}C NMR signals for **3** and **4** are consistent with other NHC-supported [Ir(COD)Cl] complexes.[63,85]

Scheme 1. Syntheses of **3**−**6**[a]

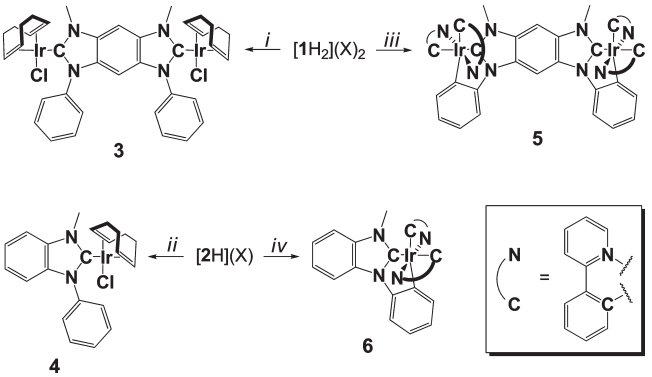

[a] (*i*) and (*ii*): X = $MeSO_4^-$, 1.0 equiv $NaN(SiMe_3)_2$ and 0.5 equiv [Ir(COD)Cl]$_2$ per NHC-unit; (*iii*) and (*iv*): X = I^-, 2.0 equiv Ag_2O and 0.5 equiv [Ir(ppy)$_2$Cl]$_2$ per NHC-unit.

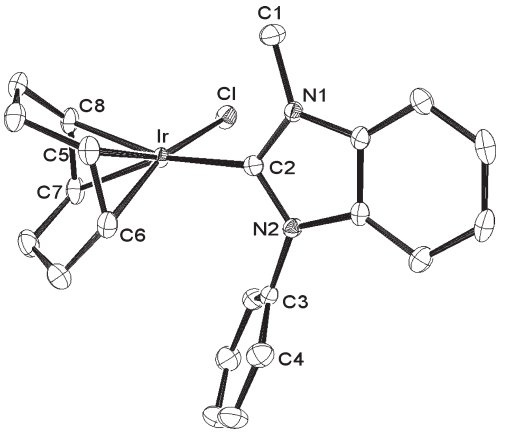

Figure 3. ORTEP diagram showing 50% probability thermal ellipsoids and selected atom labels for **4**. Hydrogen atoms have been omitted for clarity. Selected bond lengths (Å) and angles (deg): Ir−Cl, 2.3712(6); Ir−C2, 2.022(2); Ir−C5, 2.108(2); Ir−C6, 2.112(2); Ir−C7, 2.183(2); Ir−C8, 2.184(2); N1−C1, 1.456(3); N1−C2, 1.346(3); N2−C2, 1.374(3); N2−C3, 1.436(3); C2−Ir−Cl, 87.97(6); C2−Ir−C7, 158.14(9); C2−Ir−C8, 164.74 (9); Cl−Ir−C5, 156.43(7); Cl−Ir−C6, 164.31(7); N1−C2−Ir−Cl, 76.62 (19); C2−N2−C3−C4, 58.5(2). The COD bite angle is 87.3°.

Single crystals of **4** were grown from a saturated CH_2Cl_2 solution by vapor diffusion of pentane at room temperature. X-ray diffraction confirmed the structural assignment of **4** as [Ir(COD)Cl(**2**)] (Figure 3). Bond distances for Ir−Cl and Ir−C2 (2.3712(6) and 2.022(2) Å, respectively) compare well with those measured in other [Ir(COD)Cl(NHC)]

(83) Kamplain, J. W.; Lynch, V. M.; Bielawski, C. W. *Org. Lett.* **2007**, *9*, 5401–5404.

(84) Vu, P. D.; Boydston, A. J.; Bielawski, C. W. *Green Chem.* **2007**, *9*, 1158–1159.

(85) Chianese, A. R.; Mo, A.; Datta, D. *Organometallics* **2009**, *28*, 465–472.

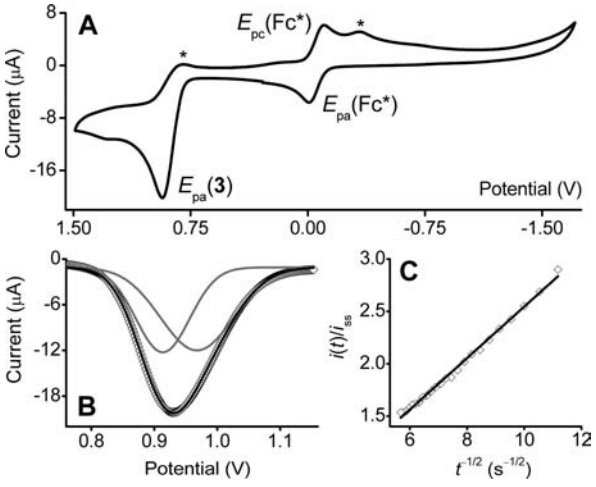

Figure 4. (A) CV of **3** with [Fc*] as an internal standard (100 mV s^{-1} scan-rate, referenced to SCE), showing a major oxidation peak (E_{pa}) and minor reduction features (*). (B) DPV of the oxidation of **3** at 0.93 V (◇) showing deconvolution into two peaks (gray lines) and the fitted peak (black line). (C) Plot of $i(t)/i_{ss}$ vs $t^{-1/2}$ data (◇) for the same oxidation and linear fit (black line, slope = 0.25, *y*-intercept = 0.069, R^2 = 0.99) allowed determination of $D_0 = 7.2 \times 10^{-6}$ cm^2 s^{-1} and n = 2.1.

Table 1. Electrochemical Properties

	E_{pa} (V)	$D_0 \times 10^5$ (cm^2 s^{-1})	n
3	0.93	0.72	2.1
4	0.95	1.9	0.91
5	0.81	1.1	2.0
6	0.79	2.6	1.2

complexes, which range from 2.335 to 2.39 Å (avg = 2.365 ± 0.012 Å) and 1.99 to 2.091 Å (avg = 2.041 ± 0.027 Å), respectively.[63,65−71] For Ir−C bonds *trans* to an NHC, the average length is 2.183±0.025 Å (range = 2.134−2.227 Å), greater than the average (2.112 ± 0.018 Å) distance for Ir−C bonds *cis* to an NHC (range = 2.081−2.155 Å). The corresponding lengths of 2.183(2) and 2.184(2) Å for the *trans* Ir−C bonds, and 2.108(2) and 2.112(3) Å for the *cis* fall outside these ranges. Presumably, the Ir−C7 and Ir−C8 bonds in **4** are longer than analogous bonds in other complexes because of a relatively strong *trans* influence from **2**. Because the bite angle of the COD ligand is highly conserved across a variety of complexes (avg = 87.1 ± 0.7°, range = 85.4−88.2°) including **4** (87.3°), any increase in *trans* Ir−C bond distances must be accompanied by a corresponding decrease in *cis* Ir−C bond distances. Relative to the [Ir(COD)Cl] plane, ligand **2** is rotated by 76.62(19)°, less than the average value of 88.8 ± 17.1° (range = 61.76−122.81°) observed for complexes of this type, but within one standard deviation.

Having attached redox active [Ir(COD)Cl] moieties to NHCs **1** and **2**, we then studied the respective complexes **3** and **4** using a variety of electroanalytical techniques; key electrochemical properties are summarized in Table 1. Cyclic voltammetry of **3** in CH_2Cl_2 revealed irreversible cathodic peaks at $E_{pc} = -0.33$ and $+0.76$ V versus SCE, with a prominent irreversible anodic peak at $E_{pa} = +0.93$ V likely arising from the $Ir^{I/II}$ oxidation (Figure 4A). Other complexes bearing [Ir(COD)Cl] moieties supported by NHCs display metal-centered oxidations at potentials ranging from 0.65 to 0.92 V, whereas NHCs with more electron-deficient N-substituents exhibit higher potentials.[63] As these substituents become more electron-deficient, the NHC can withdraw more electron density from the Ir via π-backbonding[86] and thus cause the oxidation to occur at higher potentials. Differential pulse voltammetry (DPV) for this oxidation in **3** showed only one broad peak. However, signal deconvolution revealed two overlapping peaks at +0.91 and +0.97 V of equal intensity (Figure 4B). Given this ∼60 mV separation, complex **3** appears to be a Class II compound according to the Robin-Day classification system, indicating the two metal centers are weakly electronically coupled.[64] Monoiridium complex **4** exhibited one irreversible metal-based oxidation at nearly the same potential (E_{pa} = 0.95 V); however, deconvolution of the DPV afforded only one peak.

Chronoamperometry (CA) using a Pt ultramicroelectrode facilitated measurement of the time-dependent and steady-state current, $i(t)$ and i_{ss}, of the metal-centered redox process. Plotting $i(t)/i_{ss}$ versus $t^{-1/2}$ for the oxidation of **3** enabled determination of the diffusion coefficient $D_0 = 7.2 \times 10^{-6}$ cm^2 s^{-1} and number of electrons involved n = 2.1 (Figure 4C). Because the two overlapping peaks at this potential have equal intensity, each represents a one-electron oxidation. In contrast, analysis of **4** by CA revealed $D_0 = 1.9 \times 10^{-5}$ cm^2 s^{-1} and n = 0.91, indicating that the benzimidazolylidene-bound [Ir(COD)Cl] unit undergoes a one-electron oxidation. A larger value of D_0 for **4** than **3** is expected, given that **4** is effectively the "monometallic half" of **3**.[47] From these results, we conclude that the one-electron oxidation of one iridium in **3** causes the other to occur at a potential ∼60 mV higher in energy, consistent with results previously observed for other benzobis(imidazolylidene)-linked bimetallic (Fe and Ru) complexes.[87] Because the oxidation of one iridium in **3** influences the other across bis(NHC) **1**, we hypothesized that a bimetallic complex supported by this ligand should display properties distinct from its monometallic analogue.

To complement the electrochemical analyses of **3** and **4**, we investigated their spectroscopic properties, with the key room temperature characteristics summarized in Table 2. Complex **3** displayed a highly featured absorption spectrum, with the most intense peak at 338 nm assigned as a $\pi \rightarrow \pi^*$ transition (Figure 5A). The UV−vis profile of **4** was nearly identical, with the strongest absorption occurring at 302 nm. Subtracting the absorbance spectrum of **4** from the absorbance spectrum of **3** clearly illustrates this shift, with a sharp negative peak at 302 nm and an intense positive peak at 338 nm and adjoining shoulder at 357 nm (Figure 5A inset). This 36 nm bathochromic shift in λ_{max} going from **3** to **4** is consistent with a more-delocalized π system of the former. Further evidence that the major feature is derived from the benzimidazolylidene fragment can be found by comparing the absorption spectra for [**1**H_2][$MeSO_4$]$_2$ and [**2**H][$MeSO_4$]. The absorption peak for the former is broad and maximizes at λ_{max} = 289 nm, whereas that from the latter is more structured with λ_{max} = 269 nm (Figure 5B). In the optical difference spectrum, one negative and one positive peak are observed at 269 and 289 nm, respectively (Figure 5B inset).

(86) Khramov, D. M.; Lynch, V. M.; Bielawski, C. W. *Organometallics* **2007**, *26*, 6042–6049.
(87) Mercs, L.; Neels, A.; Albrecht, M. *Dalton Trans.* **2008**, 5570–5576.

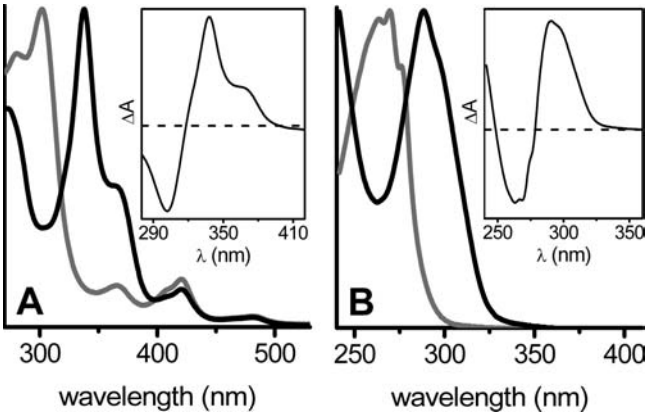

Figure 5. Normalized UV−visible absorption spectra at room temperature for: (A) complex **3** (black trace) and **4** (gray trace) in MeTHF with the optical difference spectrum for **3** minus **4** (inset, dashed line: $\Delta A = 0$); (B) $[\mathbf{1}H_2][MeSO_4]_2$ (black trace) and [**2**H][$MeSO_4$] (gray trace) in water with the difference spectrum for $[\mathbf{1}H_2][MeSO_4]_2$ minus [**2**H][$MeSO_4$] (inset, dashed line: $\Delta A = 0$).

Table 2. Room-Temperature Spectroscopic Properties[a]

	λ_{max} (nm)	$\varepsilon \times 10^{-4}$ (M^{-1} cm^{-1})	λ_{em} (nm)	Φ
$[\mathbf{1}H_2][MeSO_4]_2$[b]	289	1.45	396	0.23
[**2**H][$MeSO_4$][b]	269	1.00	396	0.046
3[c]	338	1.23	—	—
4[c]	302	1.38	—	—
5[c]	343	2.95	497	0.11
6[c]	258	5.13	497	0.19

[a] Molar extinction coefficients (ε) were determined from Beer's law plots. Quantum efficiencies (Φ) were determined relative to quinine bisulfate. [b] Measured in water under ambient conditions. [c] Measured in MeTHF under N_2 atm.

Presumably, the source of the 20 nm bathochromic shift in the $\pi \rightarrow \pi^*$ transition for $[\mathbf{1}H_2][MeSO_4]_2$ versus [**2**H][$MeSO_4$] is the same source of the 36 nm difference in the $\pi \rightarrow \pi^*$ transition energy for **4** versus **3**. Neither complex **3** nor **4** exhibited measurable phosphorescence at room temperature or 77 K, consistent with literature precedent for related NHC-supported [Ir(COD)Cl] complexes.[25] The presence of the chloride atoms could promote non-radiative decay or intersystem crossover to a non-emissive triplet excited state.[88] For example, chloride ligands have been shown to significantly depress both quantum yields and lifetimes of iridium-centered phosphorescence relative to other anionic ligands.[89]

Having studied the metal−metal and metal−ligand communication in complexes **3** and **4**, we sought to prepare analogues bearing components capable of emission, namely [Ir(ppy)$_2$] (ppy = 2-phenylpyridyl) units. Treatment of $[\mathbf{1}H_2][I]_2$ or [**2**H][I] with Ag_2O and $[Ir(ppy)_2(\mu\text{-}Cl)]_2$ in 1,2-dichloroethane afforded $[\{Ir(ppy)_2\}_2(\mathbf{1})]$ (**5**) and $[Ir(ppy)_2(\mathbf{2})]$ (**6**), respectively (Scheme 1). Theoretically, complex **5** could exist as a mixture of many isomers (*cis* or *trans* pyridyls, Λ or Δ metal centers, etc.). In the $[Ir(ppy)_2(\mu\text{-}Cl)]_2$ precursor, the ppy ligands display a *trans*-N arrangement, a configuration often preserved during complexation reactions.[90−92]

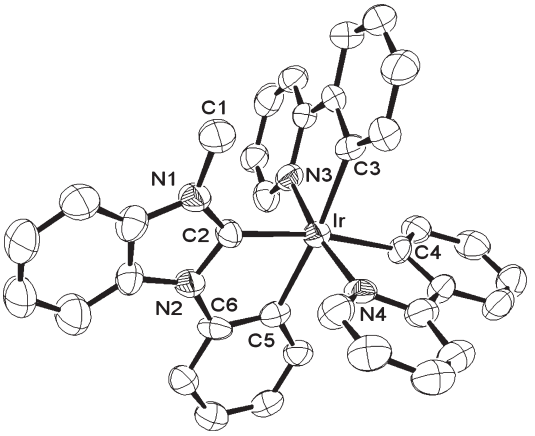

Figure 6. ORTEP diagram showing 50% probability thermal ellipsoids and selected atom labels for **6**. Hydrogen atoms have been omitted for clarity. Selected bond lengths (Å) and angles (deg): Ir−N3, 2.056(7); Ir−N4, 2.051(7); Ir−C2, 2.064(8); Ir−C3, 2.096(9); Ir−C4, 2.067(8); Ir−C5, 2.111(8); N1−C1, 1.458(12); N1−C2, 1.352(11); N2−C2, 1.373(10); N2−C6, 1.439(10); N3−Ir−N4, 171.0(3); C2−Ir−C4, 171.0 (3); C3−Ir−C4, 90.4(3); C3−Ir−C5, 174.0(3); C2−N2−C6−C5, 179.4(10).

Unfortunately, all efforts to obtain single crystals of complex **5** have been unsuccessful; however, X-ray quality crystals were obtained through slow evaporation of a saturated solution of **6** in hexanes/ethyl acetate (3:1 v/v). Structural analysis confirmed the retention of the *trans*-pyridyl configuration from the $[Ir(ppy)_2(\mu\text{-}Cl)]_2$ precursor (Figure 6). Furthermore, no significant bond length differences were observed between ligands **2** in complexes **4** or **6**, despite the rotation of the N-phenyl group into the NHC plane and formation of an organometallic bond therein. The Ir−C2 bond in **6** was ~0.04 Å longer than that in **4**, presumably because of the *trans*-influence of the Ir−C4 bond. In addition, the N-phenyl substituent had rotated from 58.5(2)° in **4** to become nearly coplanar (179.4 (10)°) with the benzimidazolylidene in **6**. No equivalent of **6** is known, but homoleptic analogues *mer*-[Ir(**2**)$_3$][28] and *mer*-[Ir(tpy)$_3$][61] (tpy = 2-(*p*-tolyl)-pyridyl) have been structurally characterized. The Ir−C2 and Ir−C5 bond distances of 2.064(8) and 2.111(8) Å, respectively, are ~0.03 Å greater than the corresponding average values in *mer*-[Ir(**2**)$_3$] (2.031 and 2.088 Å, respectively),[28] presumably a consequence of the *trans*-aryl ligands. Additionally, the C2−Ir−C5 angle of 77.9(3)° is nearly identical to the average bite angle of 78.3° in *mer*-[Ir(**2**)$_3$]. Similarly, the average Ir−C_{ppy} and Ir−N_{ppy} bond lengths observed in **6** (2.082 and 2.054 Å, respectively) compare well with those that in *mer*-[Ir(tpy)$_3$] (2.061 and 2.087 Å, respectively).[61] In addition, the N3−Ir−N4 and C3−Ir−C4 angles (171.0(3)° and 90.4(3)°, respectively) are in good agreement with the *trans*-N and *cis*-C angles in *mer*-[Ir(tpy)$_3$] (171.1° and 92.8°, respectively). Presumably, the Ir−C3 and Ir−C5 bond lengths of 2.096(9) Å and 2.111(8) Å are slightly

(88) Lakowicz, J. R. *Principles of Fluorescence Spectroscopy*, 3rd ed.; Springer: New York, 2006.
(89) Yang, L.; Okuda, F.; Kobayashi, K.; Nozaki, K.; Tanabe, Y.; Ishii, Y.; Haga, M.-a. *Inorg. Chem.* **2008**, *47*, 7154–7165.
(90) Lepeltier, M.; Lee, T. K. M.; Lo, K. K. W.; Toupet, L.; Le Bozec, H.; Guerchais, W. *Eur. J. Inorg. Chem.* **2005**, 110–117.
(91) Lo, K. K. W.; Chung, C. K.; Zhu, N. Y. *Chem.—Eur. J.* **2003**, *9*, 475–483.
(92) Neve, F.; Crispini, A.; Campagna, S.; Serroni, S. *Inorg. Chem.* **1999**, *38*, 2250–2258.

larger than the Ir−C4 bond (2.067(8) Å) because of mutual *trans*-influence. Overall, the metric parameters of **6** are in good agreement with those of its closest analogues *mer*-[Ir-(**2**)$_3$] and *mer*-[Ir(tpy)$_3$].

Structures for other *trans*-pyridyl [Ir(ppy)$_2$(L$_n$)] complexes have been obtained for a variety of ancillary ligands (L$_n$) other than NHCs.[15,37,56,59,61,62,93−106] Lengths observed for Ir−C$_{ppy}$ bonds range from 1.938 to 2.067 Å (avg = 2.00± 0.02 Å) and from 2.01 to 2.084 Å for Ir−N$_{ppy}$ bonds (avg = 2.04±0.01 Å). The corresponding average distances observed in **6** (2.082 and 2.054 Å, respectively) compare well with these values. Both the C3−Ir−C4 and N3−Ir−N4 angles in **6** (90.4(3)° and 171.0(3)°, respectively) are very close to the average values for *cis*-C$_{ppy}$ of 89.3 ± 2.9 (range = 82.0−95.2°) and for *trans*-N$_{ppy}$ of 173.9 ± 2.1 (range = 169.2−177.8°). Some variation in the topology of **6** can be measured, most likely because of of the *trans*-influence of the aryl groups, but the overall metric parameters are highly representative of Ir complexes bearing benzimidazolylidene or ppy ligands.

With evidence that the *trans*-pyridyl configuration is conserved upon NHC binding, we conclude that each iridium center in **5** will feature *trans*-pyridyls and thus can have either Λ or Δ stereochemistry. Four possible permutations of complex **5** can be drawn that satisfy these criteria, but the C_2-symmetric Λ,Λ configuration forms an enantiomeric pair with Δ,Δ. Furthermore, the Λ,Δ isomer has C_s symmetry and is the same as Δ,Λ. Consequently, **5** will be a mixture of only *two* distinguishable components: the Λ,Λ/Δ,Δ enantiomeric pair and the *meso* Λ,Δ diastereomer. Although the ^{1}H NMR spectrum for **5** exhibits extremely complex aryl features, the N-methyl groups are well-separated from this region at δ = 3.35 ppm ($CDCl_3$) and are diagnostic for benzimidazolylidenes. Two overlapping N-methyl peaks were observed for an analytically pure sample of **5**, confirming the presence of the C_2 enantiomeric pair and C_s diastereomer in roughly a 1:1 ratio. All attempts to separate these isomers via crystallization or column chromatography were unsuccessful; therefore, all measurements of **5** were performed on this mixture. Isomeric resolution in a non-carbenoid diiridium system has been achieved by anion metathesis with a chiral salt followed by chromatography, but the room temperature emission spectra of the individual isomers were identical.[39] Additionally, our electrochemical and phosphorescence measurements (vide infra) suggest that the metal centers in **5** are electronically isolated from each other, and thus their properties depend only on their ligand set and not their absolute stereochemistry.

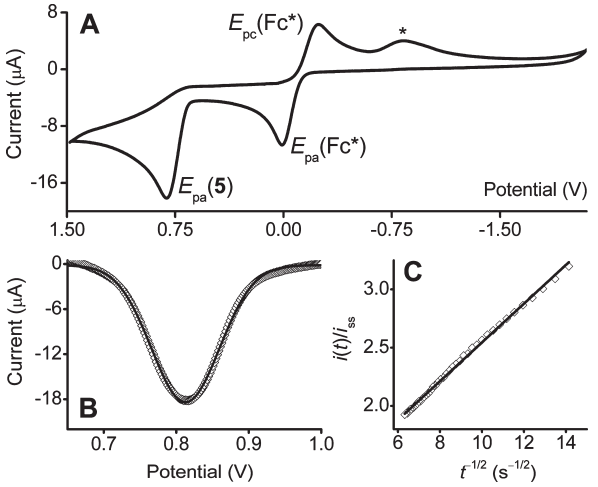

Figure 7. (A) CV of **5** with [Fc*] as an internal standard (100 mV s^{-1} scan-rate, referenced to SCE), showing a major oxidation peak (E_{pa}) and minor reduction feature (*). (B) DPV of the oxidation of **5** at 0.81 V (◇) showing deconvolution into two peaks (gray lines) and the fitted peak (black line). (C) Plot of $i(t)/i_{ss}$ vs $t^{-1/2}$ data (◇) for the same oxidation and linear fit (black line, slope = 0.17, y-intercept = 0.882, R^2 = 0.99) allowed determination of D_0 and n.

After determining the structural composition of **5** and **6**, we then investigated their electrochemical properties, whose key characteristics are summarized in Table 1. As observed with **3**, the CV of **5** showed an irreversible reduction at E_{pc} = −0.73 V and an irreversible oxidation at E_{pa} = +0.81 V, tentatively assigned as the Ir$^{III/IV}$ couple (Figure 7A). Deconvolution of the DPV for this oxidation revealed only one peak (Figure 7B), suggesting the redox events at one metal center do not influence those of the other and that complex **5** is therefore a Class I compound. Despite comprising the same bridging ligand **1**, electronic communication between iridium centers occurs in complex **3** but not complex **5**. One possible explanation is that the metal-centered orbitals in **5** are too low in energy for effective overlap with **1**, whereas those in **3** are a better match. Increasing the overlap between the frontier orbitals on the metal and the bis(NHC) will increase the degree of interaction and intermixing. As a result, the electronic environment at the metal will be more sensitive to changes in the electron density of the bis(NHC), such as the oxidation state of the distal metal.

As observed for **4**, an irreversible oxidation for **6** was observed at nearly the same potential as its bimetallic analogue (0.79 V), whose deconvoluted DPV also contained only one peak. No complexes directly equivalent to **5** or **6** are known, but the oxidation of [Ir(ppy)$_2$(acac)] (acac = 2-acetylacetonate) occurs at roughly 0.83 V,[62] consistent with the diminished electron-donating ability of acac versus an NHC. For the purely homoleptic *mer*-[Ir(ppy)$_3$], this potential shifts to 0.75 V,[61] slightly lower than the values observed for **5** and **6**. Presumably, the greater electron-donating ability of pyridine versus benzimidazolylidene lowers the Ir$^{III/IV}$ oxidation potential.

Plotting the values of $i(t)/i_{ss}$ versus $t^{-1/2}$ obtained by CA for the oxidation of **5** revealed $D_0 = 1.1\times10^{-5}$ cm^2 s^{-1} and n = 2.0

(93) Fu, H.; Ding, Y.; Chen, G. *Acta Crystallogr. E* **2008**, *64*, m731.
(94) Graf, M.; Gancheva, V.; Thesen, M.; Krüger, H.; Mayer, P.; Sünkel, K. *Inorg. Chem. Commun.* **2008**, *11*, 231–234.
(95) Li, W.-Y.; Mao, L.-S.; Lu, L.; He, H.-W. *Acta Crystallogr. E* **2008**, *64*, m490.
(96) Sie, W.-S.; Jian, J.-Y.; Su, T.-C.; Lee, G.-H.; Lee, H. M.; Shiu, K.-B. *J. Organomet. Chem.* **2008**, *693*, 1510–1517.
(97) Zhao, Q.; Li, L.; Li, F.; Yu, M.; Liu, Z.; Yi, T.; Huang, C. *Chem. Commun.* **2008**, 685–687.
(98) Chen, L.-Q. *Acta Crystallogr. E* **2007**, *63*, m2078.
(99) Han, L.-P.; Li, B.; Liu, J.; Ying, J. *Acta Crystallogr. E* **2007**, *63*, m2031–m2032.
(100) Kappaun, S.; Eder, S.; Sax, S.; Mereiter, K.; List, E. J. W.; Slugovc, C. *Eur. J. Inorg. Chem.* **2007**, 4207–4215.
(101) Kim, T.-J.; Lee, U. *Acta Crystallogr. E* **2006**, *62*, m2244–m2245.
(102) Yi, C.; Cao, Q.-Y.; Yang, C.-J.; Huang, L.-Q.; Wang, J. H.; Xu, M.; Liu, J.; Qiu, P.; Gao, X.-C.; Li, Z.-F.; Wang, P. *Inorg. Chim. Acta* **2006**, *359*, 4355–4359.
(103) Lau, M.-K.; Cheung, K.-M.; Zhang, Q.-F.; Song, Y.; Wong, W.-T.; Williams, I. D.; Leung, W.-H. *J. Organomet. Chem.* **2004**, *689*, 2401–2410.
(104) Wang, Y.; Teng, F.; Tang, A.; Wang, Y.; Xu, X. *Acta Crystallogr. E* **2005**, *61*, m778–m780.
(105) DeRosa, M. C.; Mosher, P. J.; Yap, G. P. A.; Focsaneanu, K.-S.; Crutchley, R. J.; Evans, C. E. B. *Inorg. Chem.* **2003**, *42*, 4864–4872.
(106) Marsh, R. E.; Kapon, M.; Huc, S.; Herbstein, F. H. *Acta Crystallogr. B* **2002**, *58*, 62–77.

Table 3. Luminescence Properties of **5**−**6**[a] and **I**−**IV** at Room Temperature and 77 K[b]

	RT					77 K			
	λ_{em} (nm)	Φ	τ (μs)	$k_{nr} \times 10{-}4$ (s−1)	$k_r \times 10^{-5}$ (s^{-1})	λ_{em} (nm)	Φ	τ (μs)	$k_{nr} \times 10^{-5}$ (s^{-1})
5	497	0.11	0.79	1.1	1.7	482	0.45	3.4	1.6
6	497	0.19	0.69	1.2	2.8	482	0.87	3.0	0.44
I[28]	390	0.002	0.015	65	1.3	380	0.31	2.4	2.9
II[26]	460	0.22	0.22	3.5	10	—	—	—	—
III[61]	512	0.036	0.15	6.4	2.4	493	∼1	4.2	low
IV[62]	516	0.34	1.6	0.41	2.1	—	0.67	3.2	1.0

[a] Measured in MeTHF under N_2 atmosphere. [b] Quantum efficiencies (Φ) at room temperature were determined relative to quinine bisulfate. Radiative (k_r) and non-radiative (k_{nr}) decay rates at room temperature determined by lifetime measurements. Values of Φ and k_{nr} at 77 K estimated as described in Experimental Section.

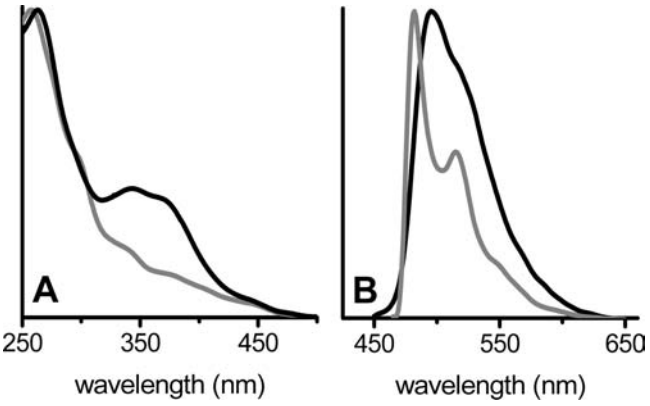

Figure 8. (A) Normalized UV−visible absorption spectra at room temperature for complex **5** (black trace) and **6** (gray trace) in MeTHF. (B) Normalized emission spectra for **5** at room temperature (black line) and at 77 K (gray line) in MeTHF.

(Figure 7C). Analysis of **6** by CA allowed determination of $D_0 = 2.6 \times 10^{-5}$ cm^2 s^{-1} and $n = 1.2$, which compare well to those observed for **4**. Because both metal-based one-electron oxidations in **5** occur at the same potential, we conclude that the two iridium centers in **5** are non-interacting. Furthermore, because this oxidation is nearly identical to that in **6** and *mer*-[Ir(ppy)$_3$],[61] we conclude that the metals are electrochemically dominated by their ppy ligands. Given that the emission from complexes of these ligands typically involves metal-to-ligand charge-transfer (MLCT), the spectroscopic properties of **5** and **6** should be very similar.

With the knowledge of electronic communication in **5** and **6** gained by electroanalytical methods, we then studied their spectroscopic properties at room temperature and 77 K; key data are summarized in Tables 2 and 3. Complex **5** displayed a broad set of absorption peaks centered at 343 nm and an intense absorption at 264 nm, whereas **6** exhibited only one broad peak at 258 nm and several weak shoulders (Figure 8). As observed with **3** and **4**, the difference in the optical profiles of **5** and **6** presumably arises from the difference in $\pi \rightarrow \pi^*$ transition wavelength inherent to the NHC scaffold. Whereas **3** was non-luminescent, the ppy analogue **5** displayed emission at 497 nm (Φ = 0.11), identified as phosphorescence by lifetime measurements (τ = 0.79 μs). Complex **6** displayed emission at the same wavelength and with the same peakshape as **6**, albeit with greater efficiency (Φ = 0.19) and shorter lifetime (τ = 0.69 μs). Upon exposure to oxygen, the phosphorescence from both **5** and **6** was rapidly quenched to immeasurable levels. Indistinguishable emission wavelengths for the mono- and bimetallic complexes are expected, given

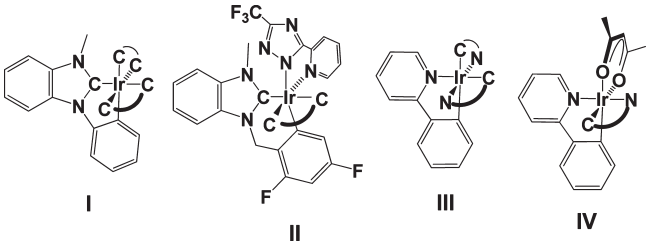

Figure 9. Homo- and heteroleptic NHC and ppy complexes.

the nearly identical electrochemical characteristics. These results demonstrate that the two [Ir(ppy)$_2$] units in **5** are non-interacting. Because the non-radiative decay rates k_{nr} of **5** and **6** are similar (1.1 and 1.2×10^6 s^{-1}, respectively), the lower quantum yield and longer lifetime of **5** are primarily due to a slower radiative decay rate k_r (1.7 vs 2.8×10^5 s^{-1} for **5** vs **6**, respectively). Collectively, these results suggest that the phosphorescence of **5** and **6** originates solely from the [Ir(ppy)$_2$] fragments, whereby the benzimidazolylidene ligands perturb the symmetry-forbidden emissive relaxation rates without altering the phosphorescence energies.

At 77 K, the broad phosphorescence observed from **5** at room temperature becomes structured, with maximum emission at λ_{max} = 482 nm. In addition, the emission lifetime (τ = 3.4 μs) exhibited a 4-fold increase with respect to the value obtained at room temperature. Assuming k_r as temperature-independent, Φ^{77} and $k_{nr}{}^{77}$ can be estimated as 0.45 and 1.6×10^5 s^{-1}, respectively. Complex **6** displayed an emission profile identical to **5** at 77 K, with similar increases in τ and Φ (3.0 μs and 0.87, respectively). The smaller non-radiative decay rate for **6** than **5** (0.44 vs 1.6×10^5 s^{-1}, respectively) at 77 K, despite being nearly equivalent at room temperature, suggests that thermal motion contributes more to non-radiative decay in **6** than in **5**. Qualitatively, this hypothesis is supported by the CA analyses, wherein the diffusion coefficient for the bimetallic complex is smaller than that for the monometallic complex. As observed at room temperature, the phosphorescence wavelength and peakshape at 77 K were independent of the nature of the imidazolylidene ligand bound to the [Ir(ppy)$_2$] fragments. Only the excited state decay was influenced by replacing **1** with **2**.

To place these luminescence results in greater context, we compared our observations of **6** to known homoleptic and heteroleptic complexes bearing NHC and ppy ligands (see Figure 9 and Table 3). Homoleptic NHC analogue *mer*-[Ir(**2**)$_3$] exhibits weak emission at ∼390 nm, with Φ = 0.002 and τ = 15 ns, when measured at room temperature

(**I**, Figure 9).[28] These values correspond to values for k_r and k_{nr} of 1.3×10^5 and 6.5×10^7 s^{-1}, respectively. Upon cooling to 77 K, the emission maximum shifts to ~380 nm, and the peak becomes structured, with the lifetime increasing to 2.4 μs ($k_{nr} = 2.9 \times 10^5$ s^{-1}). For a heteroleptic complex with two NHC ligands (**II**), emission occurs at 460 nm, with a quantum efficiency of 0.22 and a lifetime of 0.22 μs, corresponding to values for k_r and k_{nr} of 1.0 and 3.5×10^6 s^{-1}, respectively.[26] When compared with **I** and **II**, complex **6** shares more features with the latter, particularly with respect to Φ and k_{nr}. However, the radiative decay rate inherent to **I** and emissive lifetime at 77 K are closer to the values measured for **6**. Although the difference in ligands between **I** and **II** precludes detailed analysis, a general trend can be inferred: as the number of NHCs coordinated to Ir decreases, the rates of radiative decay increase and non-radiative decay decrease.

At the other extreme, homoleptic ppy analogue *mer*-[Ir(ppy)$_3$] (**III**, Figure 9) displays a broad luminescence profile at room temperature that maximizes at 512 nm, with corresponding values for Φ and τ of 0.036 and 0.15 μs, respectively.[61] Thus, the underlying radiative and non-radiative decay rates are 2.4×10^5 and 6.4×10^6 s^{-1}, respectively. In a 77 K MeTHF glass, the emission peak becomes structured and undergoes a slight hypsochromic shift to 493 nm. Under these conditions, the lifetime increases dramatically to 4.2 μs, and the quantum yield approaches unity. For the heteroleptic derivative with two ppy ligands [Ir(ppy)$_2$(acac)] (**IV**), room temperature phosphorescence is observed at 516 nm, with $\Phi = 0.34$ and $\tau = 1.6$ μs, whereby the latter increases to 3.2 μs at 77 K.[62] These measurements indicate $k_r = 2.1\times10^5$ s^{-1} and $k_{nr} = 4.1 \times 10^5$ s^{-1} at room temperature (1.0×10^5 s^{-1} at 77 K). Between **III** and **IV**, complex **6** exhibits photophysical properties (i.e., Φ, τ, k_r) that compare well with those of the latter. A trend is observed for the ppy-based complexes similar to that with the NHC analogues, whereby going from **III** to **IV** affords a dramatic increase in quantum yield and lifetime, primarily because of the decrease in non-radiative decay rate.

Of the homoleptic and heteroleptic NHC- and ppy-based complexes presented in Figure 9, complex **6** is most similar to [Ir(ppy)$_2$(acac)]. Therefore, we believe that the [Ir(ppy)$_2$] components in **5** and **6** are effectively functioning as insulated emissive units, whereby coordination of **1** or **2** merely perturbs intrinsic properties without significant changes to emission energy. Because the frontier orbitals for **1** and **2** are similar, considering the emission profiles of [**1**H$_2$][MeSO$_4$]$_2$ and [**2**H][MeSO$_4$] are identical, the [Ir(ppy)$_2$] moieties in **5** and **6** are perturbed in similar ways and therefore exhibit identical phosphorescence profiles.

Conclusions

Two new bimetallic Ir complexes supported by 1,7-dimethyl-3,5-diphenylbenzobis(imidazolylidene) (**1**) were synthesized and compared with monometallic analogues bearing 1-methyl-3-phenylbenzimidazolylidene (**2**). Although electrochemical analyses of [{Ir(COD)Cl}$_2$(**1**)] (**3**) demonstrated the oxidation of one [Ir(COD)Cl] unit influenced the other (ΔE = ~60 mV), no such interaction was observed between the [Ir(ppy)$_2$] moieties in [{Ir(ppy)$_2$}$_2$(**1**)] (**5**). This lack of electronic communication was also observed in the phosphorescence of **5**, whose emission profile was superimposable with that of its monometallic analogue, [Ir(ppy)$_2$(**2**)] (**6**), with the only distinction arising from their different decay rates. We believe the electronic communication in the Ir(I) complex **3** and lack thereof in the Ir(III) complex **5** are consequences of greater bis(NHC)−ML$_n$ orbital overlap in **3** than in **5**, owing to the better match in energy levels between **1** and [Ir(COD)Cl] than **1** and [Ir(ppy)$_2$].

We initially pursued complex **5** to determine the extent of metal−metal electronic communication across ditopic bis(NHC) **1** and how this interaction affected the luminescent properties (e.g., emission wavelength, quantum yield, lifetime, etc.) but were surprised that no such communication was observed. Because the emission energies of **5** and **6** were identical, we conclude that benzimidazolylidene coordination to an [Ir(ppy)$_2$] fragment neither perturbs the emissive state nor facilitates interaction between units thereof. Thus, multiple units could be chained together with derivatives of **1** without altering the fundamental phosphorescence energy or peakshape inherent to the fundamental [Ir(ppy)$_2$] unit.

On the basis of these observations, we believe that novel phosphorescent materials could be obtained via incorporation of known MLCT-phosphors into bimetallic or polymeric systems with bis(NHC)s functioning as non-interfering molecular connectors, an invaluable tool in the emerging fields of nano- and molecular electronics.[107] Essentially, a monometallic complex [(ML$_n$)L′] (where ML$_n$ is the MLCT chromophore and L′ is exchangeable with an NHC) would be selected from known phosphors or prepared de novo for desired phosphorescence characteristics. Then, a multimetallic complex or organometallic CMP could be prepared, without altering the emission wavelength, by linking multiple ML$_n$ units with a multitopic NHC: the non-interfering molecular connector. We believe this novel strategy could facilitate the rational design of new phosphorescent materials from established phosphors, as well as second-generation bimetallic dopants, for use in a wide variety of optoelectronic applications.

Acknowledgment. We are grateful to the NSF (CHE-0645563), the ONR (N00014-08-1-0729), the Robert A. Welch Foundation (F-1621), and the Arnold and Mabel Beckman Foundation for their generous financial support of this work. C.W.B. is a Cottrell Scholar of Research Corporation. M.S.C. is grateful to the University of Texas at Austin for an Undergraduate Research Fellowship. We would also like to thank Alec Nepomnyashchii and Joaquin Rodriguez Lopez for invaluable electrochemical assistance and insightful discussions.

Supporting Information Available: ^{1}H and ^{13}C NMR spectra of [**1**H$_2$][I]$_2$, [**2**H][I], [**2**H][MeSO$_4$], and **3**−**6**; electrochemical data for **3**−**6**; emission spectra for **6**; X-ray crystallographic data, including tables, ORTEP diagrams, and CIF files for **4** and **6**. This material is available free of charge via the Internet at http://pubs.acs.org.

(107) Robertson, N.; McGowan, C. A. *Chem. Soc. Rev.* **2003**, *32*, 96–103.